Functional analyses of cellulose synthase genes in flax (Linum usitatissimum) by virus-induced gene silencing

Maxime Chantreau, Brigitte Chabbert, Sylvain Billiard, Simon Hawkins, Godfrey G. Neutelings

Plant Biotechnology Journal

Plant Biotechnology Journal (2015) **13**, pp. 1312–1324 doi: 10.1111/pbi.12350

Functional analyses of cellulose synthase genes in flax (*Linum usitatissimum*) by virus-induced gene silencing

Maxime Chantreau[1], Brigitte Chabbert[2,3], Sylvain Billiard[4], Simon Hawkins[1] and Godfrey Neutelings[1,*]

[1]*UMR INRA 1281 Stress Abiotiques et Différenciation des Végétaux Cultivés, Université Lille Nord de France Lille 1, Villeneuve d'Ascq, France*

[2]*INRA, UMR 614 Fractionnement des AgroRessources et Environnement, Reims, France*

[3]*UMR 614 Fractionnement des AgroRessources et Environnement, Université de Reims Champagne-Ardenne, Reims, France*

[4]*UMR CNRS 8198 Laboratoire de Génétique & Evolution des Populations Végétales, Université Lille Nord de France Lille 1, Villeneuve d'Ascq, France*

Received 27 April 2014;
revised 5 January 2015;
accepted 8 January 2015.
**Correspondence* (Tel 33 0 320 434 029;
email godfrey.neutelings@univ-lille1.fr)

Keywords: cellulose, fibres, flax, gene expression, silencing, virus-induced gene silencing.

Summary

Flax (*Linum usitatissimum*) bast fibres are located in the stem cortex where they play an important role in mechanical support. They contain high amounts of cellulose and so are used for linen textiles and in the composite industry. In this study, we screened the annotated flax genome and identified 14 distinct cellulose synthase (*CESA*) genes using orthologous sequences previously identified. Transcriptomics of 'primary cell wall' and 'secondary cell wall' flax *CESA* genes showed that some were preferentially expressed in different organs and stem tissues providing clues as to their biological role(s) *in planta*. The development for the first time in flax of a virus-induced gene silencing (VIGS) approach was used to functionally evaluate the biological role of different *CESA* genes in stem tissues. Quantification of transcript accumulation showed that in many cases, silencing not only affected targeted *CESA* clades, but also had an impact on other *CESA* genes. Whatever the targeted clade, inactivation by VIGS affected plant growth. In contrast, only clade 1- and clade 6-targeted plants showed modifications in outer-stem tissue organization and secondary cell wall formation. In these plants, bast fibre number and structure were severely impacted, suggesting that the targeted genes may play an important role in the establishment of the fibre cell wall. Our results provide new fundamental information about cellulose biosynthesis in flax that should facilitate future plant improvement/engineering.

Introduction

The *Linum* genus contains about 180 different species spread across the six continents (Sveinsson *et al.*, 2014). Some of these species have been exploited by man since at least the upper Palaeolithic period when wild flax fibres were used by hunter-gatherers to make cords (Kvavadze *et al.*, 2009). Common flax (*Linum usitatissimum*) was then domesticated during the Neolithic era and became one of the earliest cultivated plants used for weaving (Zohary and Hopf, 2004) but also as an oil source (Oomah, 2001). Since then, commercial flax has been progressively selected to optimize stem content in cellulose-rich phloem fibres (bast fibres) and/or seed oil naturally rich in omega-3 alpha-linolenic acid (ALA).

Bast fibres are very long cells located beneath the epidermis in the stem cortex of some plants such as flax, hemp, ramie and jute (Huis *et al.*, 2012). They are considered among the longest cells in terrestrial plants where they can reach up to 55 cm in ramie (*Boehmeria nivea*) (Aldaba, 1927). These fibres are characterized by a very thick secondary cell wall (CWII) generally containing high amounts of crystalline cellulose, significant amounts of hemicellulose and low lignin contents in contrast to the much more heavily lignified cell walls typically found in the xylem tissue of most plants (Day *et al.*, 2005b; Gorshkova and Morvan, 2006; Neutelings, 2011; Chantreau *et al.*, 2014). In addition to their particular chemical composition, the bast fibre CWII is also characterized by parallel cellulose microfibrils aligned with respect to the fibre axis thereby conferring tensile strength (Gorshkova *et al.*, 2012). This special composition and organization of cell wall polymers explains the particular physical properties of these fibres that are used in the textile (linen) industry and more recently in composite materials for the car and aeronautic industries Day et al., 2013.

In plants, cellulose microfibrils are believed to contain 36 glucan chains, each one synthesized by an individual cellulose synthase (CESA) subunit organized in a heteromeric rosette complex (CSC) in which the exact number of units is still uncertain (Somerville, 2006). CESAs are part of the CAZy glycosyltransferase family 2 (GT2) and catalyse the polymerization of ß-(1,4) glucans using UDP-glucose as a substrate. They are large proteins bound to the plasma membrane by 8 transmembrane helices with a cytosolic region containing the D_D_D_QxxRW motif involved in catalytic activity. They belong to a large protein superfamily including nine additional subfamilies named cellulose synthase-like (CSL) defined by sequence similarity to CESAs. Different *CESA* genes are generally believed to be more specifically associated with either primary or secondary cell wall cellulose biosynthesis. In fact while cellulose is present in both the primary and secondary plant cell wall, the two wall types show important differences in the degree of polymerization and crystallinity (Lei *et al.*, 2012). In *Arabidopsis,* there are 10 *CESA* genes; three different CESAs (CESA4, 7 and 8) are needed to synthesize the cellulose microfibrils in CWII, while in the primary cell wall, the CSCs contain CESA1 and 3 and CESA6-like isoforms (CESA2, 5, 6 and 9). The role of AtCESA10 is less clear. When sequences from other plant species are included for phylogenetic analyses, six clades can be highlighted (Nairn and Haselkorn, 2005). Three of these clades are suspected to include the CWII-associated CESAs

with each clade containing at least one *CESA* gene from each species. Among the 3 remaining 'primary cell wall clades', one contains the family three sequences, the second contains AtCESA1 and AtCESA10, and the last clade contains AtCESA2, 5, 6 and 9.

Given the cellulose-rich nature of the flax bast fibre cell wall and the importance of this polymer in determining fibre performance and quality, there are surprisingly only few reports on *CESA* genes in this species (Galinousky *et al.*, 2014; Mokshina *et al.*, 2014). The practical interest of such an investigation for flax is underlined by a recent study demonstrating that a functional relationship exists between CESA structures, cellulose crystallinity and saccharification efficiency in *Arabidopsis* (Harris *et al.*, 2012). While the information available from the recently sequenced genome of *Linum usitatissimum* (Wang *et al.*, 2012) has already been used to describe some cell wall-related gene families in this species (Barvkar *et al.*, 2012; Babu *et al.*, 2013; Hobson and Deyholos, 2013; Mokshina *et al.*, 2014), no studies have yet undertaken a functional approach on members of the *CESA* gene family.

Currently, functional genomics of a high number of genes in flax are difficult to carry out using a standard transgenic approach. Although stable transgene integration has been successfully performed in this species, the plant transformation rate remains low and obtaining regenerated plants is a time-consuming process (Caillot *et al.*, 2009). For this reason, a gene inactivation approach by VIGS (virus-induced gene silencing) (Baulcombe, 2006) is an interesting alternative because this technique is relatively easy to implement on many different plant species (Senthil-Kumar and Mysore, 2011). VIGS utilizes the naturally occurring phenomenon of post-transcriptional gene silencing (PTGS) that is believed to derive from an ancient mechanism involved in the defence of host cells against foreign nucleic acids, including viruses and active transposable elements (Voinnet, 2009). In the VIGS approach, a fragment of the targeted gene is cloned into a modified viral vector inserted in a plasmid. The viral DNA is then delivered to the plant by *Agrobacterium tumefaciens* infection. The most popular and efficient vector is the bi-partite TRV-VIGS vector (Liu *et al.*, 2002; a) derived from the tobacco rattle virus, a member of the genus *Tobravirus*. The TRV vectors are the most commonly used and have been tested successfully on at least a dozen of different species (Tian *et al.*, 2014). As VIGS vectors derive from plant viruses, the success of the gene silencing depends on the compatibility between the virus and the host plant. *Linum usitatissimum* has been reported to be susceptible to TRV (Brunt *et al.*, 1996), and in this paper, we report the use of this vector to induce silencing of flax *CESA* genes.

Results

Characterization and expression of flax *CESA* genes

Flax *CESA* genes were identified by BLAST screening the annotated genome (Wang *et al.*, 2012) and published (Day *et al.*, 2005a; Fenart *et al.*, 2010; Venglat *et al.*, 2011) or unpublished (http://www.ncbi.nlm.nih.gov) EST sequences followed by manual inspection. Altogether, we identified 14 potential *LusCESA* genes based on their homology to orthologous characterized sequences (Figure 1). The *in silico* characterization of the genomic sequences showed that a mistake occurred in the annotation of *Lus10008225* and *Lus10008226* which were considered as two short genes separated by a 361 nt fragment. This was probably due to an inappropriate splicing design resulting from a stretch of unknown nucleotides present on the scaffold_157. Both sequences were associated and compared to the sequenced ESTs to remodel the splice junctions. We obtained the *Lus10008225-6* genomic sequence of 4193 bp resulting in a predicted protein of 1057 amino acids (Figure 1).

These results confirm the data recently published by Mokshina *et al.* (2014) during the revision of this manuscript. These authors identified 14 *CESA* genes based on the published flax genome, as well as two additional genes (*CESA7A*, *CESA7B*) on the scaffolds 57 and 464, thereby bringing the potential total number of flax *CESA* genes to 16. However, inspection of the CESA7A protein structure showed that it was missing 2 transmembrane domains, and we therefore re-aligned flax ESTs (Fenart *et al.*, 2010) and genomic data from Phytozome to generate a complete flax CESA7 protein (Figure 1). Similarly, the proposed CESA7B protein lacks an N-terminal Zn domain and is most likely a CSL protein, rather than a true CESA. These observations seem to show that the flax genome only contains a single *CESA7* gene as indicated in another recent paper (Galinousky *et al.*, 2014). Taken together, our results suggest that the flax genome contains 15 *CESA* genes (Figure 1).

The predicted *LusCESA* genes (Figure 1) have a size ranging from 3867 to 5836 bp and contain 11 to 14 exons which form coding regions between 2721 and 3294 bp (906 to 1097 amino acids). All the resulting proteins show characteristic features of plant CESAs (Delmer, 1999; Saxena *et al.*, 2001) including a Zn-binding motif and two transmembrane domains in the N-Terminal region, a central domain with a class-specific region and a GT2 motif (D_D_D_QxxRW) and finally six C-terminal transmembrane domains. A phylogenetic tree containing the protein sequences from *Arabidopsis thaliana, Populus trichocarpa* and *Linum usitatissimum* (Figure 2) shows that the 15 flax CESA genes are separated into 6 different clades in agreement with recently published data (Mokshina *et al.*, 2014).

Previous studies indicate that the genes involved in the formation of either the primary or secondary cell wall rosette structure are coexpressed in *Arabidopsis* (Persson *et al.*, 2005) and in rice (Wang *et al.*, 2010). To get a first overview of the potential functions of the flax *CESA* genes identified in this study, we determined the expression profiles of three genes from 'primary cell wall' clades (*LusCESA1-A*, *LusCESA3-C* and *LusCESA6-E*) and two genes from 'secondary cell wall' clades (*LusCESA4* and *LusCESA8-B*). Samples were collected at four different heights in the flax stem representing a developmental gradient from young (sample 1, upper) to older (sample 4, lower) stem tissues (Figure 3a). Stem samples from positions 2, 3 and 4 were separated into outer tissues (rich in bast fibres) and inner tissues (mainly xylem). *CESA* gene expression was also evaluated in the flowers, leaves and roots (Figure 3b). *LusCESA1-A* and *LusCESA6-D* showed very similar expression profiles. For both genes, no significant differences could be detected between inner- and outer-stem tissues regardless of stem height. Both genes were expressed in flowers, leaves and roots but at lower levels than in stem tissues. On the other hand, both *LusCESA4* and *LusCESA8-B* were more highly expressed in the inner stem tissues compared to the outer-stem tissues. Both genes were only very weakly expressed in flowers, leaves and roots. Interestingly, *LusCESA3-C* showed an opposite expression profile to *LusCESA4* and *LusCESA8-B* with significantly higher expression in outer-stem tissues even though this difference was reduced at the bottom of the stem. In

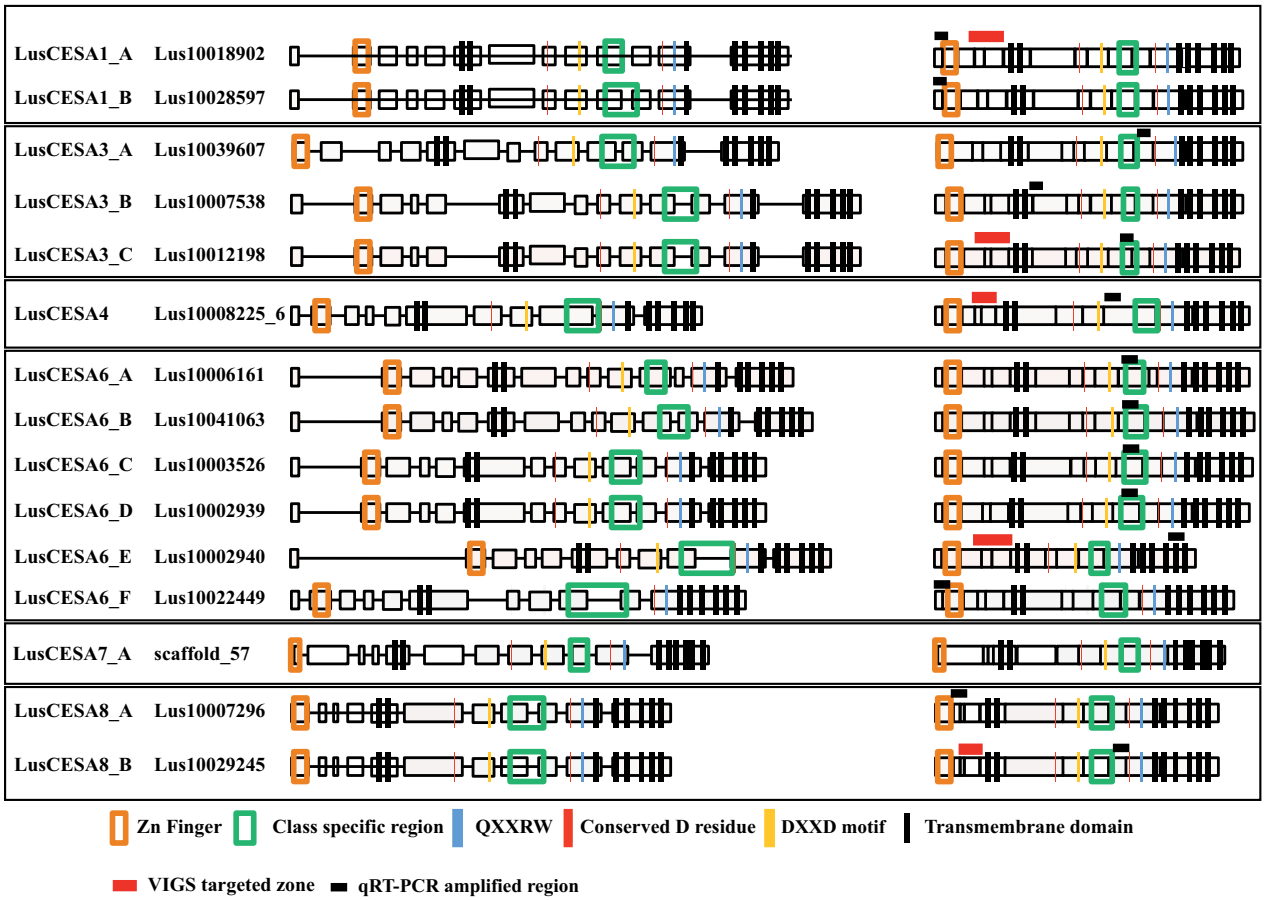

Figure 1 Gene structure of the 15 flax *CESA* genes. The genomic sequence (left) and predicted coding sequence (right) structures are shown with the CESA characteristics. Exons are represented by boxes and introns by lines.

flowers, leaves and roots, *LusCESA3-C* showed a similar expression to *LusCESA1-A* and *LusCESA6-D*.

Induction and optimization of TRV-based silencing in flax

To optimize VIGS in flax, different infection procedures (Table 1) were tested using a 450-bp cDNA fragment of *LusPDS* (Phytozome: Lus10021967) cloned into TRV2 and introduced in *Agrobacterium*. The *PDS* gene encodes a phytoene desaturase required for the biosynthesis of chlorophyll-protecting carotenoids (Kumagai *et al.*, 1995). Silencing of *PDS* genes leads to an easily detectable photobleaching phenotype (Ruiz *et al.*, 1998), and they are therefore often used as positive controls in VIGS. Of the different tested protocols, agrodrench, carborundum abrasion and infection with preamplified virus particles in tobacco only gave very low efficiency values. The number of photobleached plants increased when they were soaked in the bacterial suspension under vacuum, but the best results were obtained by syringe infection. Developmental stages and density of *Agrobacterium* inoculum are known to impact the efficiency of VIGS in some species (Velasquez *et al.*, 2009), and so we also evaluated these parameters. Plants were infected at 12, 15 and 20 days after germination with suspensions containing increasing bacterial densities (OD_{600} = 0.5; 1; 1.5 and 2), but no significant differences in silencing phenotypes were observed (data not shown). Slight virus infection symptoms appeared 13 days postinoculation (dpi), and the first photobleached leaves and stems were visible 24 dpi (Figure 4a,d). When plants were infected with nonrecombinant TRV vectors, leaves exhibited only very mild wrinkling and occasional small pale zones (Figure 4c). No impact was observed on flax stems.

In other species, weak phenotypes have been associated with uneven virus distribution between the main stem and lateral branches (e.g. peanut stripe potyvirus, PStV) (Jain *et al.*, 2000). In tobacco, topping of plants resulted in a more efficient spread of the virus in the leaves of lateral shoots produced from the activated axillary buds (Wijdeveld *et al.*, 1992). We therefore removed the shoot apical meristem just after *Agrobacterium* inoculation in an attempt to improve the systemic spread of the virus. The plants then developed two secondary basal shoots 3 days after apex removal. These conditions led to a much higher silencing efficiency (up to 95%, see Table 1) and a more rapid (8 dpi versus 13 dpi) and generalized appearance of photobleached zones. This observation would suggest that the latent period associated with apex removal allows improved viral multiplication before lateral shoot regrowth.

Silencing of flax cellulose synthase genes

To explore the role of the flax *CESA* genes using a VIGS approach, we constructed independent recombinant TRV2 vectors containing sequences specific to the 3 'primary' (clades 1, 3 and 6) and 2 'secondary' (clades 4 and 8) cell wall *CESA* genes analysed in this

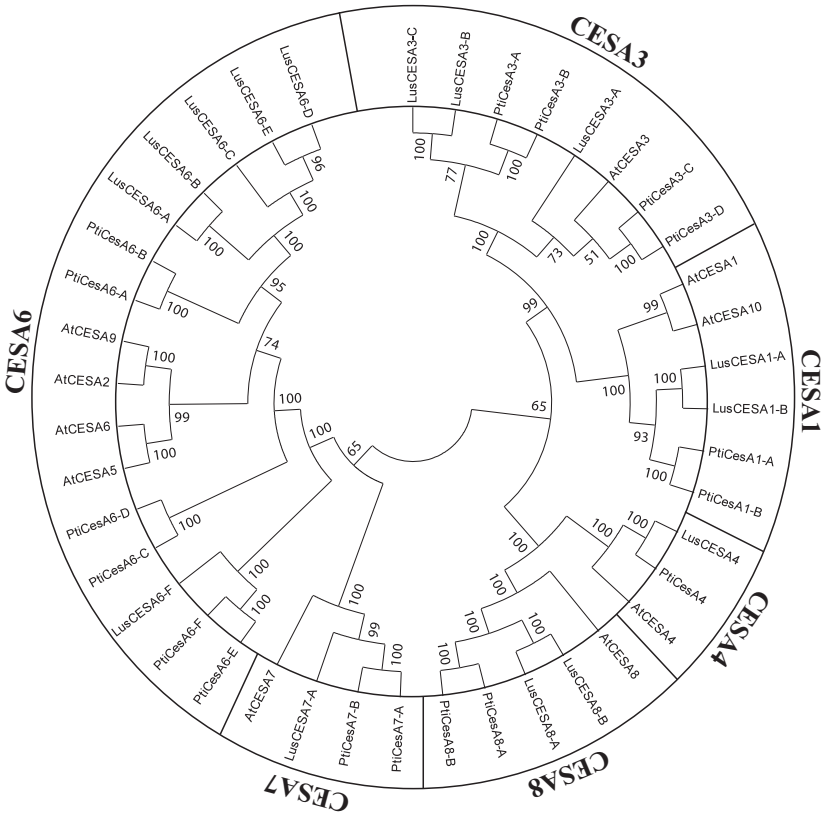

Figure 2 Neighbour-joining phylogenetic tree of CESA proteins. *Arabidopsis thaliana* (At), *Populus trichocarpa* (Pti) and *Linum usitatissimum* (Lus) sequences of the CESA superfamily were aligned with ClustalW (Thompson *et al.*, 1994) and the tree created with MEGA5 (Tamura *et al.*, 2011). Bootstrap values over 50% of 500 replications are indicated in the nodes.

study. These sequences (Figure 1) corresponded to the structurally heterogeneous N-terminal region located between the zinc finger and the first transmembrane domain of the CESA protein (Somerville, 2006) and allowed us to theoretically distinguish between the different clades. At the same time, the similarity between different CESA genes in the same clade also allowed us to use a single vector to target all genes within a given clade (Table S1). The 5 vectors were then used to infect flax plants that were named V_CS1, V_CS3, V_CS4, V_CS6 and V_CS8, respectively.

Expression of 14 *LusCESA* genes was evaluated by qRT-PCR in individual axillary stems of infected plants harvested at 35 dpi (Figure 5) and compared to the empty vector controls. The melting curves of all final products were carefully inspected to check that only one fragment was amplified with each primer couple (Table S2). Of the 14 tested *LusCESA* genes, all were expressed at detectable levels except for *LusCESA6-A* and *LusCESA6-F*. When an appropriate vector targeted a specific clade, expression levels of the corresponding genes were always significantly lower when compared to the control (100%), except for *LusCESA3-A* and *LusCESA3-C* (V_CS3 plants) and *LusCESA4* (V_CS4 plants). In the case of the V_CS3 silenced plants, this was not due to the time of sampling as the expression of the 2 genes was not significantly lower at 10, 21 and 31 days after the infection (Figure S1). Specific transcript level decreases varied from 24% (*LusCESA3-B*) to 74% (*LusCESA6-C*), respectively, and were >47% for clades 1, 6 and 8. Interestingly, when a specific *CESA* clade was targeted, at least one other gene outside this clade was also affected except in the case of V_CS3 plants. For example, when clade 1 or clade 8 CESAs were targeted, the mRNA levels of all *LusCESA* genes were significantly reduced compared with control plants. Similarly, the targeting of clade 6 *CESAs* affected all clades except for the clade 1. On the contrary, the only effect observed when the clade 4 was targeted was a 35% reduction in *LusCESA6-E* transcripts. In some cases, the reduction in transcript accumulation for a given gene was lower with the clade-specific vector than with other nonspecific vectors. For example, the reduction in the expression of the *LusCESA8-A* gene was greater in V_CS1 (58%) and V_CS6 (74%) plants when compared to V_CS8 plants (47%).

Phenotypic analyses of *CESA*-silenced plants

At 35 dpi, all silenced plants were smaller than the controls (Figure 6a). A curly leaf phenotype was also visible in V_CS1, V_CS3 and V_CS6 plants (Figure 6b). To see whether stem anatomy and cell wall formation were affected in silenced plants, we examined thin transverse stem sections stained with toluidine-blue-O (TBO). In agreement with the observed reduction in plant size, all stem sections contained fewer secondary xylem cell layers and a complete pith region. More modifications were observed in V_CS1, V_CS3 and V_CS6 plants (Figure 7) than in V_CS4 and V_CS8 plants (data not shown). *CESA* gene silencing had a marked effect on outer-stem tissues in both V_CS1 and V_CS6 plants. This effect was particularly strong in V_CS1 plants (Figure 7c,d) where the outline of cortical parenchyma cells was highly irregular and epidermal cells appeared more rounded than in control plants (Figure 7a). Bast fibre number was greatly reduced, and cell shape was irregular. Vascular cambial cells and young differentiating xylem cells, but not more mature lignified xylem cells, were also characterized by an irregular cell contour. Dense purple-coloured deposits were observed between pith cells and probably represent cell wall material of crushed cells. In V_CS3 plants (Figure 7e,f), the overall cell shape was much less affected and outer-stem tissues appeared normal with no marked modifications to bast fibre number and shape. In contrast, an important effect was observed at the xylem–pith junction where

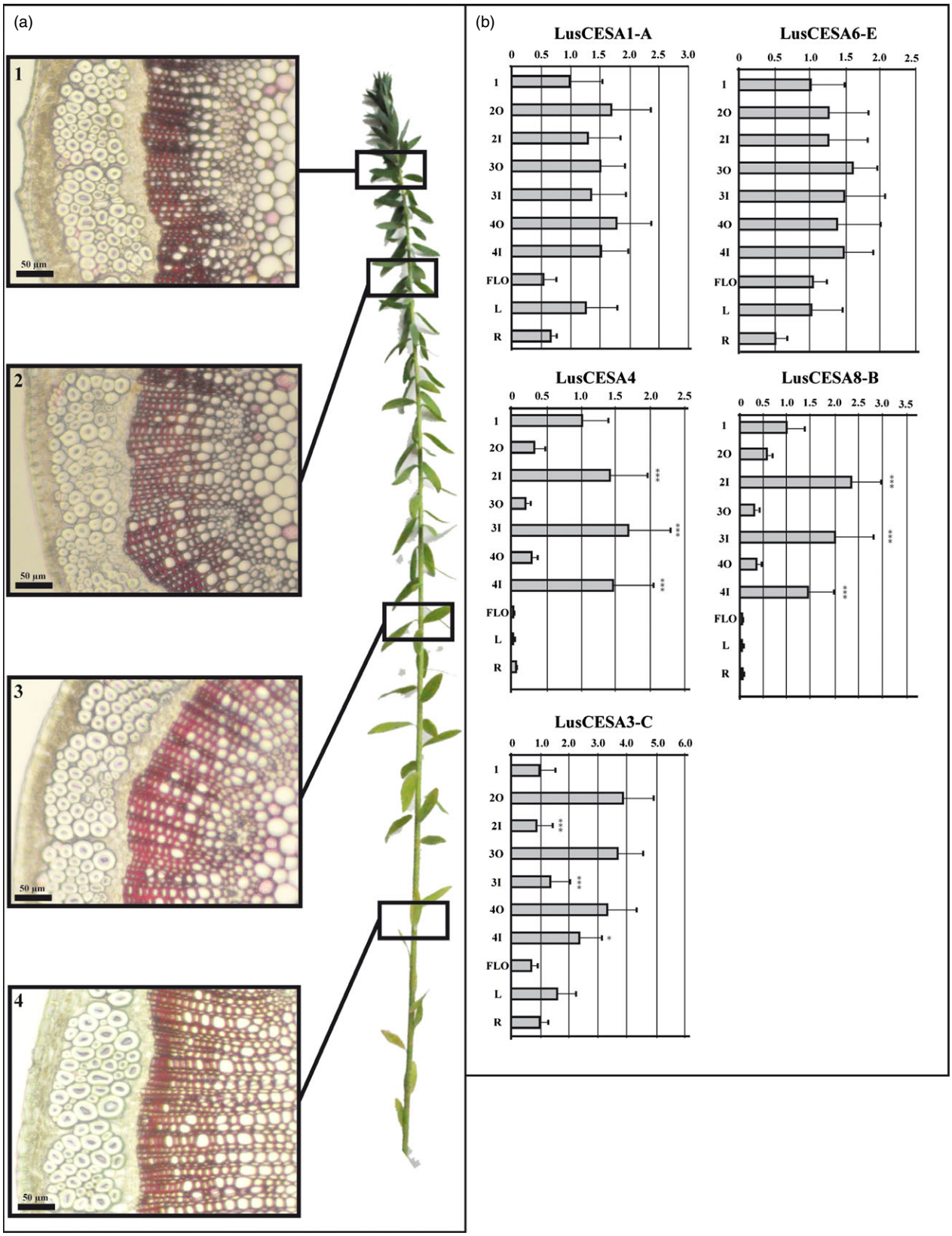

Figure 3 Clade-specific gene expression in flax stems at different heights. (a): Four flax wild-type stem fragments were collected, and transversal sections were stained with phloroglucinol-HCl. The lignified cell walls are coloured in red. (b): Relative quantification of a member from 5 CESA clades by qRT-PCR. The value of the top whole fragment (1) was set to 1. The numbers 1, 2, 3 and 4 indicate the position of each fragment (4, 10, 25 and 40 cm from the shoot apex, respectively) as shown in (a). I: Inner tissues; O: outer tissues; FLO: flower buds; L: leaves; R: roots. Significant differences between the outer and inner tissues were shown at $P < 0.001$ (***),$P < 0.01$ (**) and $P < 0.05$ (*). Mean expression values and standard deviation were presented.

Table 1 Virus-induced gene silencing-induced PDS silencing with previous published protocols

Infection method	Number of tested plants	Infection efficiency (% infected flax plants)	Protocol reference
Agrodrench	63	0%	(Ryu *et al.*, 2004)
Abrasion	56	2%	(Ruiz *et al.*, 1998)
Sap inoculation	15	20%	(Brigneti *et al.*, 2004)
	55	0%	(Valentine *et al.*, 2004)
Vacuum	39	72%	(Hileman *et al.*, 2005)
Syringe	39	85%	(Fu *et al.*, 2005)
Syringe (removed apical meristem)	95	95%	This paper

numerous lignified cells appeared to be crushed and/or showed irregular outlines. The impact of *CESA* silencing was most extreme in V_CS6 plants where an important disorganization was observed (Figure 7g–i). The secondary xylem ring was incomplete although small poles of primary xylem containing 2–3 lignified cells could be observed in certain zones. In outer tissues, the epidermis was unaffected, but the cortical parenchyma was highly disorganized with very irregular blue-coloured deposits of cell wall material. Similar deposits could also be observed at the xylem–pith interface. As for V_CS1 plants, bast fibre number was greatly reduced.

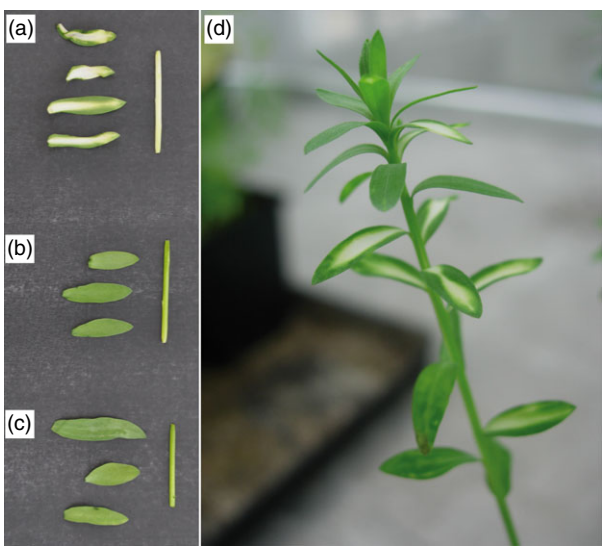

Figure 4 Phenotype of the TRV2-*PDS*-transformed plants. (a): Leaves and a stem fragment of a photobleached plant. (b): The same organs from a wild-type plant and (c): from an empty vector control-transformed plant. (d): Young lateral stem emerging from a TRV2-*PDS*-transformed plant.

An analysis of the sugar content was also performed to identify potential differences in the cell wall composition between the control and silenced plants (Figure 8). *CESA* silencing produced significant modifications in sugar composition. Slight but significant reductions in the relative proportion of glucose were determined in V_CS1 (8.6%), V_CS3 (10.5%) and V_CS6 (14.4%) plants compared to the control group. Modifications in sugar content associated with other cell wall polymers were also observed. The most important impact was observed in V_CS6 plants where the rhamnose content increased by 200% and the galactose and galacturonic acid content increased by 160% ($P < 0.001$). Significant increases for these sugars were also observed in V_CS1 and V_CS3 plants. In contrast, xylose content remained constant in all VIGS infiltrated plants.

Discussion

In flax, the role of the bark is not only to protect the plant against outside attacks but also to confer rigidity to the stem. This latter property is fundamental to prevent lodging because the ratio between the length and the width of the stem can reach values close to 400 in cultivated *Linum* species. The stem rigidity is reinforced by the outlying bast fibres organized in bundles, each one containing tens of elementary units cemented together by pectins (Charlet *et al.*, 2010). At the end of their development process, their CWII are very well developed and are usually larger than the cell lumen itself. The presence of high amounts of cellulose is an extremely important feature of these cell walls, and engineering/breeding of flax plants for better fibre quality requires an improved understanding of the mechanisms controlling its synthesis.

Based on the flax published genome (Wang *et al.*, 2012) and re-evaluation of recent data (Mokshina *et al.*, 2014), we identified 15 gene models that meet the criteria described in previously characterized CESA sequences, that is the presence of specific motifs such as an N-terminal zinc finger, 8 transmembrane domains and a class-specific region (Richmond and Somerville, 2000). The 15 flax *CESA* genes could be assigned to 6 different clades as observed in other plant species (Carroll and Specht, 2011; Yoo and Wendel, 2014).

Analyses of flax *CESA* gene expression from 'primary' and 'secondary' cell wall clades revealed a number of organ-specific differences. Of particular interest is the observation that *LusCESA3-C* was much more highly expressed in outer-stem tissues containing bast fibres than in inner stem tissues. A similar, but less important, difference in the expression of this gene was also recently observed in these tissues (Mokshina *et al.*, 2014). While it is tempting to speculate that this gene (and/or other clade 3 genes) may play a specific role in the synthesis of the bast fibre cell wall, further characterization is necessary. Organ-/tissue-specific differential expression of *CESA* genes is also supposed to be related to cell wall formation in cellulose-rich cotton fibres. In this species, a clade 1 gene, *GhCESA6,* is more highly expressed in the cotton bolls as compared to the stem (Li *et al.*, 2013) and may therefore have a more important role in the construction of the cell wall of cotton fibres (single cell outgrowths of seed epidermal cells) as compared to other CESA genes involved in xylem cell wall formation. In contrast to the higher expression of the *LusCESA3-C* gene in outer-stem tissues, 2 other genes (*LusCESA4* and *LusCESA8-B*) were more highly expressed in inner stem tissues in agreement with recently published results (Mokshina *et al.*, 2014). This study also reported a similar expression pattern for the flax *CESA7* gene clade, and it is

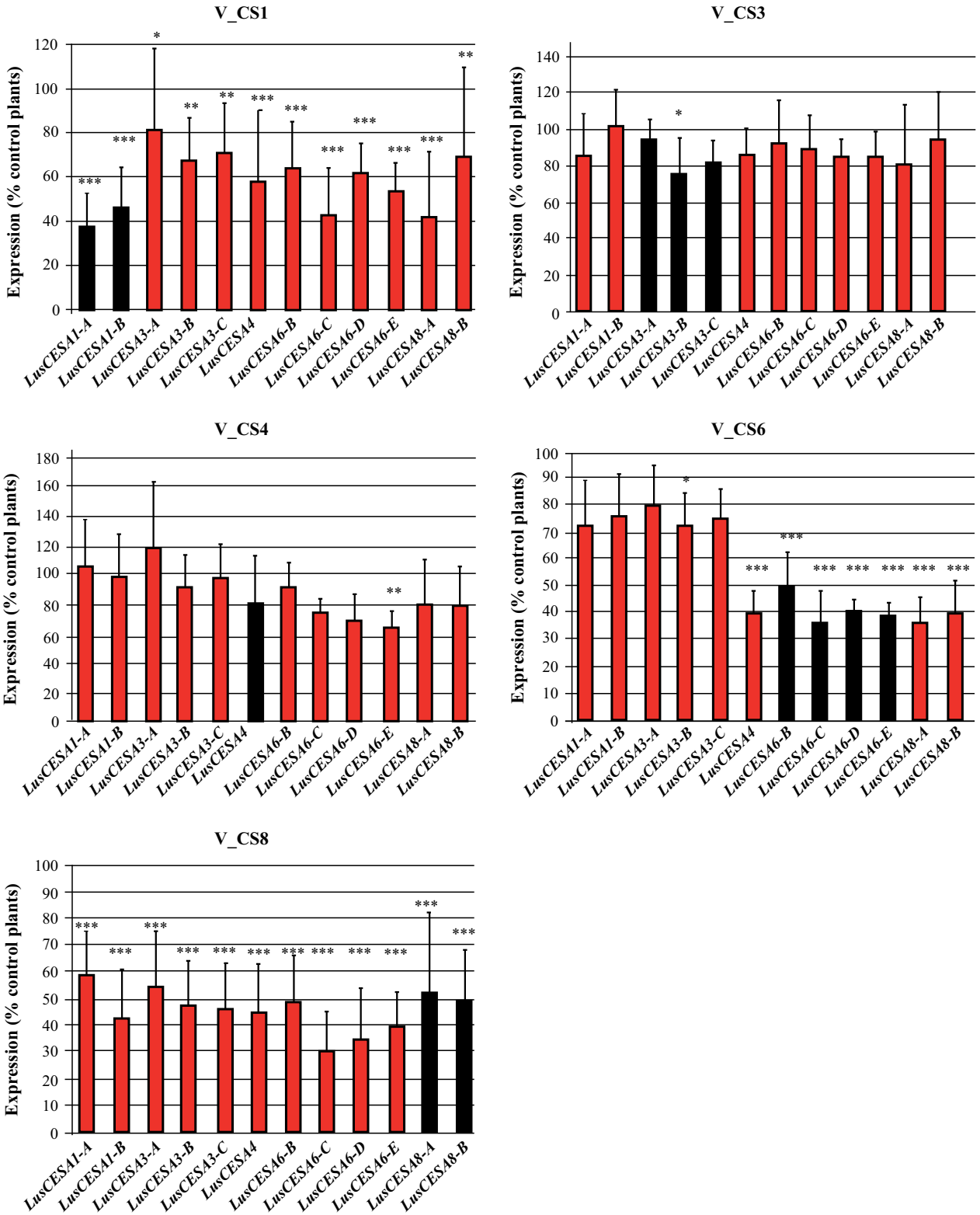

Figure 5 qRT-PCR analysis of *LusCESA* genes in TRV2-*CESA*-transformed plants. The number associated with the V_CS nomenclature indicates the corresponding clade-specific fragment. The bars indicating the genes targeted by VIGS are in black. Significant differences between the transformed and the control plants were shown at $P < 0.001$ (***),$P < 0.01$ (**) and $P < 0.05$ (*). Mean expression values and standard deviation were presented.

likely that these 3 flax clades (*LusCESA4*, *LusCESA8* and *LusCESA7*) are functional orthologs of the CWII-specific *AtCESA4*, *AtCESA7* and *AtCESA8* genes in *Arabidopsis*.

The role of different flax *CESA* genes in cell wall metabolism was then functionally characterized by a reverse genetics approach. In flax, functional genomics is hampered because

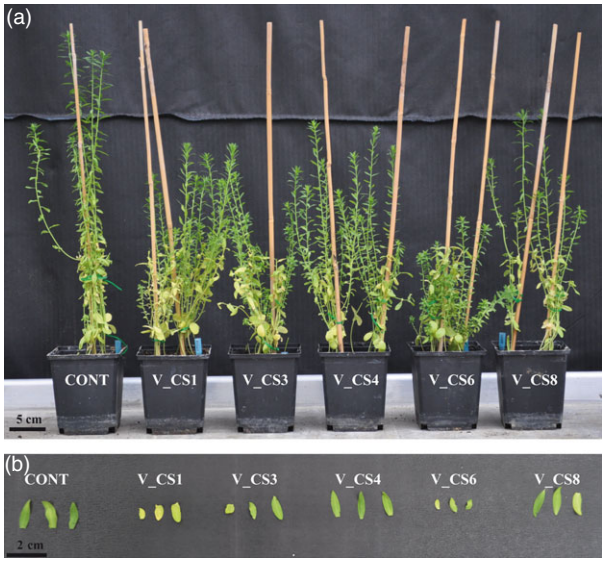

Figure 6 Phenotype of the TRV2-*CESA*-transformed plants. (a): Plant height; (b): leaf form/size. The number associated with the V_CS nomenclature indicates the corresponding clade-specific fragment. CONT: empty vector control.

stable transformation is time-consuming. We therefore decided to see whether we could develop a VIGS protocol for this species. To our knowledge, this is the first report of successful gene knock-down in the *Linaceae* family by this method. Previous published data reported an interaction between the oat blue dwarf virus and *Linum usitatisimum* (Banttari and Zeyen, 1972), but no VIGS vector has been constructed from this genome. In other plant species, the TRV vector system (Liu *et al.*, 2002) has been widely used because of its large host spectrum. Flax was reported to be susceptible to TRV in the Virus Identification Data Exchange project (Brunt *et al.*, 1996), and we therefore used this vector to silence selected *LusCESA* genes. We first used a flax *PDS* gene as a positive control because silencing causes a photobleaching phenotype due to the inhibition of carotenoid biosynthesis (Kumagai *et al.*, 1995). Initial testing of different infection protocols revealed that syringe infiltration of young leaves with an equal mix of TRV1 and recombinant TRV2 was the most efficient. In our first attempts, we noticed that bleached leaves were distant from the origin of infection and that silencing only spreads to a limited number of leaves and only poorly to the stem. However, when the apex of the plant was removed, the two secondary shoots that developed at the bottom of the stem immediately gave rise to organs with a strong bleached phenotype. This protocol enabled us to obtain plants showing modified gene expression at only 3 weeks after germination as compared to the average time (>3 months) necessary to select stably transformed transgenic lines. The observed photobleaching of stem cortical chlorenchyma confirmed that *PDS* silencing was also effective in this organ, indicating that VIGS can be considered as a quick and simple method for screening several cell wall genes within stem bast fibres. This approach could also be used to functionally characterize other key genes in flax. For example, flax seeds are considered as major sources of polyunsaturated fatty acids used as feed and food products and also contain high amounts of the biologically active lignan secoisolariciresinol diglucoside (SDG), and it would therefore be interesting to use the VIGS approach to investigate these metabolic pathways. VIGS has indeed already been successfully achieved on seeds or grains of several crop species such as *Triticum* and *Physalis* (Ma *et al.*, 2012; Zhang *et al.*, 2014).

For the VIGS silencing of flax *CESA* genes, we constructed 5 vectors that targeted 3 'primary' and 2 'secondary' cell wall clades. In the light of the recent identification (Mokshina *et al.*, 2014) of the flax *CESA7* gene, it would also be interesting to target this gene in future studies. Modifications in the expression of 14 identified flax *CESA* genes were then monitored by qRT-PCR. Our results indicated that targeted silencing was successful in all plants except for the clade 3 (V_CS3 plants), in which only *LusCESA3-B* was significantly down-regulated, and clade 4. The reduction in transcript abundance compared to the control was variable depending on the clade and reached 74% for *LusCESA6-C*. The efficiency of VIGS can depend on the position of the insert with respect to the cDNA (Liu and Page, 2008) and may also vary between different members of the same multigenic family even when the fragment is designed to target the same area. Our results also indicated that there was a strong cross-regulation effect between the members of the different CESA clades. This was most likely not due to homology between targeted and nontargeted sequences as the alignment of the fragments used for the constructs and the corresponding CESA sequences did not contain any identical 21 nt sequence stretches (Figure S2). For example, our results show that the silencing of the clade 8 had an effect not only on *LusCESA8-B* and *LusCESA8-A* but also on other *CESA* genes expressed in the stem. Of interest is the observation that the down-regulation of nontargeted genes may be greater than that of the targeted gene. Such an effect was seen for the two *LusCESA8* genes in V_CS6 plants, as well as for the *LusCESA6-C* in V_CS8 plants. Although a cross-suppression effect cannot be totally excluded, the identity between the sequences in clade 6 and 8 does not exceed 55% and is unlikely to directly trigger the silencing pathway. A more plausible explanation could be that of *CESA* gene co-regulation. Previous studies on the VIGS down-regulation of *CESA* genes in barley showed that expression of the closely related *CSL* genes as well as the more distantly related *GT8* gene was reduced, suggesting that the expression of several cell wall biosynthetic genes is linked with that of *CESA* (Held *et al.*, 2008). In flax, it seems likely that clade 4 and clade 8 genes are involved in CWII synthesis, but it is difficult for the moment to determine the role of other genes with respect to the synthesis of the primary or secondary cell wall. In flax, the fact that significant silencing was observed for the 3 *LusCESA3* genes in V_CS1 plants, for the *LusCESA4* in V_CS6 and for both *LusCESA8* genes in V_CS6 already allows us to outline a number of possible interactions between these clades. The amount of flax transcriptomic data is currently growing and will lead to the identification of regulatory networks of genes involved in CWII synthesis.

VIGS-induced *CESA* down-regulation in flax also provoked a visible phenotype, and all plants infected with a TRV2-*CESA* construction were markedly shorter than plants infected with the empty control vector. In the stem, our VIGS approach showed that the down-regulation of CWII orthologous genes had no phenotypic effect on the cell walls, presumably because the residual gene activities were sufficient for cell construction. The most severe impact on tissue organization was observed in V_CS6 plants, and the strongest effect on bast fibre cells occurred in V_CS1 plants. In both cases, typical CWII organization was replaced by a structure of irregular thickness that resembled a primary wall. This strong phenotype can be related to the down-

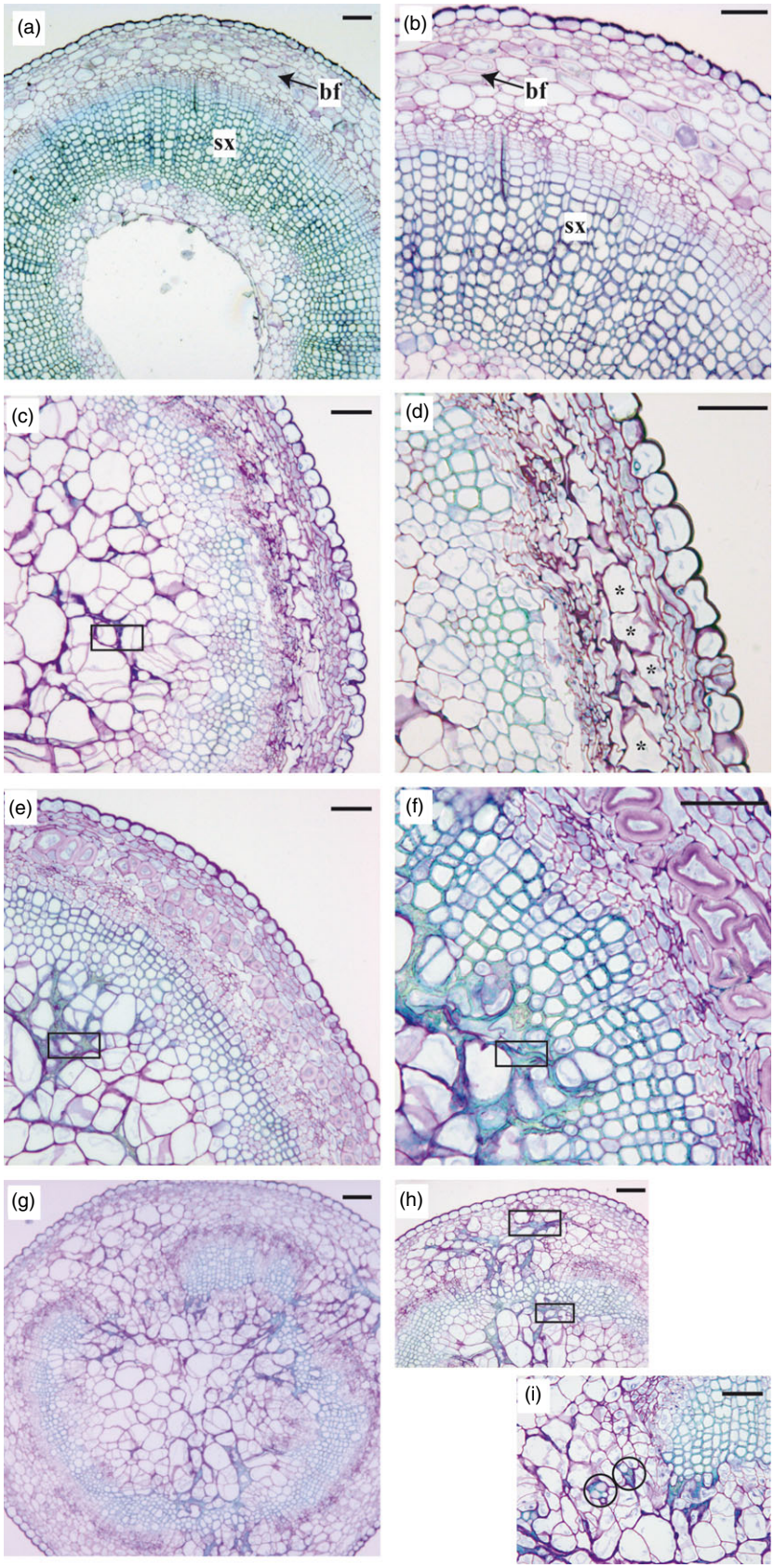

Figure 7 Cytological observation of CESA-silenced plant stems. (a–b): wild-type plants; (c–d): TRV2-*CESA1*-transformed plants; (e-f): TRV2-*CESA3*-transformed plants; (g-i): TRV2-*CESA6*-transformed plants. Square frames show collapsed/agglomerate cell walls; circles show residual primary xylem poles; asterisks shows large parenchyma cells without secondary walls in place of cellulosic fibres. sx: secondary xylem; bf: bast fibres. Bar: 50 μm.

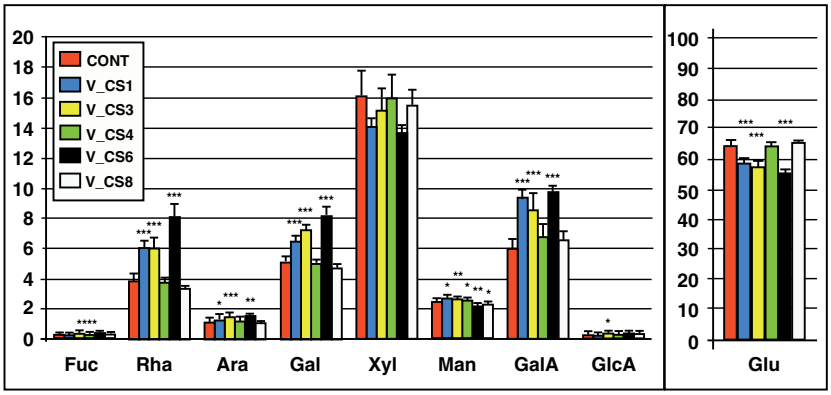

Figure 8 Sugar composition of cell wall polysaccharides in whole stems. The values are expressed as percentage ratios of each sugar to the total sugar content and are statistically compared to empty vector control plants. Significant differences between the transformed and the control plants were shown at $P < 0.001$ (***),$P < 0.010$ (**) and $P < 0.05$ (*). Mean expression values and standard deviation were presented.

regulation of all the identified *CESA* genes in these plants. Reduction in plant size was also observed when *CESA1* and *CESA3* genes were silenced by RNAi in *Arabidopsis* (Burn *et al.*, 2002) or when a *NtCesA-1* fragment was targeted by VIGS in tobacco (Burton *et al.*, 2000). In this later species, the size of the leaves was also reduced as observed in flax V_CS1, V_CS3 and V_CS6 plants. The cell shape modifications observed in the flax stem is also similar to that observed in the *Arabidopsis irx* (*cesA4-8*) mutants for Liepman *et al.* (2010). It still remains unclear whether the phenotypic modifications observed in the flax stem were only due to *CESA* down-regulation or to a global modification of co-regulated genes. Chemical analyses showed that VIGS down-regulation of *CESA* genes was associated with a slight but significant decrease in the proportion of glucose, suggesting that cellulose content was also reduced in these plants to the same extent as in VIGS silenced tobacco (Burton *et al.*, 2000) but lower than that observed in the *Arabidopsis prc-1* mutant (MacKinnon *et al.*, 2006) or the rice *Bc6* mutant (Kotake *et al.*, 2011). The observed increase in the proportion of other cell wall-related sugars also suggests that the structure/amount of noncellulosic polysaccharides (NCPs) was modified in these plants. The relatively low impact on cellulose content could be related to the propagation of heterogenous viral cDNA as previously suggested (Burton *et al.*, 2000). In the stem, virus particles are transported by the phloem and then move through the cells via the plasmodesma. It is possible that fibres located near the phloem are targeted more rapidly than the inner parts of the stem.

In conclusion, we have provided new transcriptomic and functional data on flax cellulose synthase genes. Their phylogenetic distribution is similar to that of poplar, which also belongs to the Malpighiale order. To provide functional information, we successfully developed a VIGS approach and demonstrated that the most important effect on bast fibres was obtained by targeting *CESA* genes previously described as actors of the primary cell wall formation. This may suggest that they can play an important role in the establishment of the fibre cell walls. These data will also contribute to our overall knowledge about the formation of bast fibres in other important fibre species such as ramie, jute and hemp. VIGS could also be used as a tool to explore the relationship between *CESA* genes and flax domestication by studying differential expression between cultivated flax (*L. usitatissimum*) and its wild progenitor (*L. bienne*). In addition, we are currently using this tool to target other cell wall genes identified in a mutant flax population (Chantreau *et al.*, 2013). The implementation of VIGS in this species will enhance the importance of flax as an emerging model system for studying cell wall metabolism.

Experimental procedures

Plant material

Flax plants (*Linum usitatissimum*) were grown in a greenhouse under 16 h/20 °C day and 8 h/18 °C night conditions. For microscopic, transcriptomic and sugar analyses, 43-day-old axillary stems from 3 silenced and control plants were immediately frozen in liquid nitrogen.

Light microscopy

The stem fragments were submitted to a series of alcohol baths and then embedded in methacrylate resin (Technovit 7100; Kulzer; Heraeus; Germany). Sections of 5 μm thickness were made using a microtome, stained with toluidine-blue-O and examined using a LEICA DM2000 (Leica Microsystems GmbH, Wetzlar, Germany).

Sugar analyses

Tissue samples from the pooled material were ground and repeatedly 80% ethanol extracted. Complete acid hydrolysis of cell wall polysaccharides into sugar monomers was performed using a two-step hydrolysis. Samples were swollen in 72% H_2SO_4 for 2 h at 20 °C followed by a second hydrolysis with 1 M H_2SO_4 for 2 h at 100 °C. The released monosaccharides were separated by high-performance anion-exchange chromatography (PA1 column, Dionex, Thermo Fisher Scientific, St Herblain, France using 2-deoxy-D-ribose as internal standard and standard solutions of neutral sugars and acidic sugars (Beaugrand *et al.*, 2004). One-way ANOVA was used to analyse the effect of VIGS transformation on the sugar composition at $P < 0.001$ (SigmaPlot, Systat Software, Erkrath, Germany). Multiple comparisons between transformed versus control samples (Holm–Sidak method) were then performed.

Molecular constructions

Cellulose synthase sequences from poplar and *Arabidopsis* were used to search for orthologs in the flax genome (Wang *et al.*, 2012) and in cDNA sequences obtained from the GenBank database (http://www.ncbi.nlm.nih.gov) and an EST database (Fenart *et al.*, 2010). The resulting sequences were then aligned and manually inspected. Fragments were PCR-amplified on cDNA using primers described in Table S3 and cloned into pCR2.1 plasmid using the TOPO TA cloning kit (Thermo Fisher Scientific, St Herblain, France). They were subsequently digested with *Eco*RI, purified on electrophoresis agarose gel using the QIAquick Gel Extraction kit (Qiagen, Courtaboeuf,

France) and cloned into TRV2 vector (Liu *et al.*, 2002) using T4 DNA ligase (Thermo Fisher Scientific, St Herblain, France).

Agrobacterium infiltration

TRV1 and TRV2 constructs were introduced into *Agrobacterium tumefaciens* strain GV2260 by electroporation, and the bacteria were grown in a selective LB medium supplemented with 10 mM MES and 20 mM acetosyringone and centrifuged and the pellet resuspended in an agroinfiltration medium containing 1 M $MgCl_2$, 10 mM MES and 150 μM acetosyringone. The agro-drench protocol (Ryu *et al.*, 2004) was conducted by depositing 1 mL of a 1 : 1 mixture of *Agrobacterium* solutions containing TRV1 and TRV2-PDS plasmids on the crown part of 15-day-old plants. Flax plants were also immersed in a mix of both bacterial suspensions supplemented with Silwet 0.05% and vacuum infiltrated for 5 min (Hileman *et al.*, 2005). The penetration of the agrobacterial suspensions was also maximized after sprinkling a small quantity of carborundum powder on 4 fully expanded leaves (Ruiz *et al.*, 1998). A viral multiplication was also done in *Nicotiana benthamiana* plants before infecting flax plants with a syringe. The leaf sap was collected by grinding the leaves and centrifugation of the extract followed by a precipitation step (Valentine *et al.*, 2004) or not (Brigneti *et al.*, 2004). The best results were obtained by syringe infiltration (Fu *et al.*, 2005). Using a 1-mL syringe, a 1 : 1 mixture of TRV1 and TRV2-*PDS Agrobacterium* suspension was infiltrated in the four first fully expanded leaves. The infection efficiency was further increased when the apical meristem was removed. The silencing then occurred in the two stems initiated from the lateral buds.

RNA analysis

Total RNA was extracted from isolated flax stems (three plants per experiments) as previously described (Huis *et al.*, 2010). RNA integrity was evaluated using the Experion electrophoresis system (Bio-Rad, Marnes-la-Coquette, France). For each sample, 500 ng of RNA was reverse-transcribed using the Iscript cDNA synthesis kit (Bio-Rad) according to the manufacturer's instructions. Primer pairs (Table S2) were specifically designed for the identified *CESA* gene models using Primer3 (Rozen and Skaletsky, 2000) and optimized for a Tm at 60 °C and for the amplification of 90–180 bp fragments. The qRT-PCRs were carried out in a reaction volume of 20 μL (5 μL diluted cDNAs, 10 μL of 2× SYBR Green mix and primer pairs at 0.4 μM). All PCRs were performed on three technical repetitions under the following conditions: 95 °C for 15 min, 40 cycles of 10 s at 95 °C and 30 s at 60 °C. The expression data were analysed as previously described (Huis *et al.*, 2010). We performed a generalized linear mixed model (GLMM) with the individuals as the random factor and the treatment as the fixed factors for each measured gene and for each organ separately. The procedure of model selection was followed, and the interpretation was performed as previously described (Zuur *et al.*, 2008).

Phylogenetic analysis

Phylogenetic tree of CESA proteins was made using neighbour-joining method conducted in MEGA5 (Tamura *et al.*, 2011). Bootstrap consensus tree inferred from 500 replicates. Branches corresponding to partitions reproduced <50% bootstrap replicates are collapsed. The evolutionary distances were computed using the *p*-distance method.

References

Aldaba, V.C. (1927) The structure and development of the cell wall in plants I. Bast fibers of *Boehmeria* and *Linum*. *Amer. J. Bot.* **14**, 16–22.

Babu, P.R., Rao, K.V. and Reddy, V.D. (2013) Structural organization and classification of cytochrome P450 genes in flax (*Linum usitatissimum* L.). *Gene*, **513**, 156–162.

Banttari, E.E. and Zeyen, R.J. (1972) Ultrastructure of flax with a simultaneous virus and mycoplasma-like infection. *Virology*, **49**, 305–308.

Barvkar, V.T., Pardeshi, V.C., Kale, S.M., Kadoo, N.Y. and Gupta, V.S. (2012) Phylogenomic analysis of UDP glycosyltransferase 1 multigene family in *Linum usitatissimum* identified genes with varied expression patterns. *BMC Genom.* **13**, 175.

Baulcombe, D.C. (2006) Short silencing RNA: the dark matter of genetics? *Cold Spring Harb. Symp. Quant. Biol.* **71**, 13–20.

Beaugrand, J., Cronier, D., Thiebeau, P., Schreiber, L., Debeire, P. and Chabbert, B. (2004) Structure, chemical composition, and xylanase degradation of external layers isolated from developing wheat grain. *J. Agric. Food Chem.* **52**, 7108–7117.

Brigneti, G., Martin-Hernandez, A.M., Jin, H., Chen, J., Baulcombe, D.C., Baker, B. and Jones, J.D. (2004) Virus-induced gene silencing in *Solanum* species. *Plant J.* **39**, 264–272.

Brunt, A.A., Crabtree, K., Dallwitz, M.J., Gibbs, A.J., Watson, L. and Zurcher, E.J. (1996). *'Plant Viruses Online: Descriptions and Lists from the VIDE Database.'* from http://pvo.bio-mirror.cn/refs.htm.

Burn, J.E., Hocart, C.H., Birch, R.J., Cork, A.C. and Williamson, R.E. (2002) Functional analysis of the cellulose synthase genes *CesA1*, *CesA2*, and *CesA3* in Arabidopsis. *Plant Physiol.* **129**, 797–807.

Burton, R.A., Gibeaut, D.M., Bacic, A., Findlay, K., Roberts, K., Hamilton, A., Baulcombe, D.C. and Fincher, G.B. (2000) Virus-induced silencing of a plant cellulose synthase gene. *Plant Cell*, **12**, 691–706.

Caillot, S., Rosiau, E., Laplace, C. and Thomasset, B. (2009) Influence of light intensity and selection scheme on regeneration time of transgenic flax plants. *Plant Cell Rep.* **28**, 359–371.

Carroll, A. and Specht, C.D. (2011) Understanding plant cellulose synthases through a comprehensive investigation of the cellulose synthase family sequences. *Front Plant Sci.* **2**, 5.

Chantreau, M., Grec, S., Gutierrez, L., Dalmais, M., Pineau, C., Demailly, H., Paysant-Leroux, C., Tavernier, R., Trouve, J.P., Chatterjee, M., Guillot, X., Brunaud, V., Chabbert, B., van Wuytswinkel, O., Bendahmane, A., Thomasset, B. and Hawkins, S. (2013) PT-Flax (phenotyping and TILLinG of flax): development of a flax (*Linum usitatissimum* L.) mutant population and TILLinG platform for forward and reverse genetics. *BMC Plant Biol.* **13**, 159.

Chantreau, M., Portelette, A., Dauwe, R., Kiyoto, S., Cronier, D., Morreel, K., Arribat, S., Neutelings, G., Chabi, M., Boerjan, W., Yoshinaga, A., Mesnard, F., Grec, S., Chabbert, B. and Hawkins, S. (2014) Ectopic lignification in the flax lignified bast fiber1 mutant stem is associated with tissue-specific modifications in gene expression and cell wall composition. *Plant Cell*, **26**, 4462–4482.

Charlet, K., Jernot, J.P., Eve, S., Gomina, M. and Breard, J. (2010) Multi-scale morphological characterisation of flax: from the stem to the fibrils. *Carbohydr. Polym.* **82**, 54–61.

Day, A., Addi, M., Kim, W., David, H., Bert, F., Mesnage, P., Rolando, C., Chabbert, B., Neutelings, G. and Hawkins, S. (2005a) ESTs from the fibre-bearing stem tissues of flax (*Linum usitatissimum* L.): expression analyses of sequences related to cell wall development. *Plant Biol (Stuttg).* **7**, 23–32.

Day, A., Ruel, K., Neutelings, G., Cronier, D., David, H., Hawkins, S. and Chabbert, B. (2005b) Lignification in the flax stem: evidence for an unusual lignin in bast fibers. *Planta*, **222**, 234–245.

Day, A., Fenart, S., Neutelings, G., Hawkins, S., Rolando, C. and Tokarski, C. (2013) Identification of cell wall proteins in the flax (Linum usitatissimum) stem. *Proteomics*, **13**, 812–825.

Delmer, D.P. (1999) CELLULOSE BIOSYNTHESIS: exciting times for a difficult field of study. *Annu. Rev. Plant Physiol. Plant Mol. Biol.* **50**, 245–276.

Fenart, S., Ndong, Y.P., Duarte, J., Riviere, N., Wilmer, J., van Wuytswinkel, O., Lucau, A., Cariou, E., Neutelings, G., Gutierrez, L., Chabbert, B., Guillot, X.,

Tavernier, R., Hawkins, S. and Thomasset, B. (2010) Development and validation of a flax (*Linum usitatissimum* L.) gene expression oligo microarray. *BMC Genom.* **11**, 592.

Fu, D.-Q., Zhu, B.-Z., Zhu, H.-L., Jiang, W.-B. and Luo, Y.-B. (2005) Virus-induced gene silencing in tomato fruit. *Plant J.* **43**, 299–308.

Galinousky, D.V., Anisimova, N.V., Raiski, A.P., Leontiev, V.N., Titok, V.V. and Khotyleva, L.V. (2014) Cellulose synthase genes that control the fiber formation of flax (*Linum usitatissimum* L.). *Russ. J. Genet.* **50**, 20–27.

Gorshkova, T. and Morvan, C. (2006) Secondary cell-wall assembly in flax phloem fibres: role of galactans. *Planta*, **223**, 149–158.

Gorshkova, T., Brutch, N., Chabbert, B., Deyholos, M., Hayashi, T., Lev-Yadun, S., Mellerowicz, E.J., Morvan, C., Neutelings, G. and Pilate, G. (2012) Plant fiber formation: state of the art, recent and expected progress, and open questions. *Crit. Rev. Plant Sci.* **31**, 201–228.

Harris, D.M., Corbin, K., Wang, T., Gutierrez, R., Bertolo, A.L., Petti, C., Smilgies, D.M., Estevez, J.M., Bonetta, D., Urbanowicz, B.R., Ehrhardt, D.W., Somerville, C.R., Rose, J.K., Hong, M. and Debolt, S. (2012) Cellulose microfibril crystallinity is reduced by mutating C-terminal transmembrane region residues CESA1A903V and CESA3T942I of cellulose synthase. *Proc. Natl. Acad. Sci. USA*, **109**, 4098–4103.

Held, M.A., Penning, B., Brandt, A.S., Kessans, S.A., Yong, W., Scofield, S.R. and Carpita, N.C. (2008) Small-interfering RNAs from natural antisense transcripts derived from a cellulose synthase gene modulate cell wall biosynthesis in barley. *Proc. Natl. Acad. Sci. USA*, **105**, 20534–20539.

Hileman, L.C., Drea, S., Martino, G., Litt, A. and Irish, V.F. (2005) Virus-induced gene silencing is an effective tool for assaying gene function in the basal eudicot species *Papaver somniferum* (opium poppy). *Plant J.* **44**, 334–341.

Hobson, N. and Deyholos, M.K. (2013) Genomic and expression analysis of the flax (*Linum usitatissimum*) family of glycosyl hydrolase 35 genes. *BMC Genom.* **14**, 344.

Huis, R., Hawkins, S. and Neutelings, G. (2010) Selection of reference genes for quantitative gene expression normalization in flax (*Linum usitatissimum* L.). *BMC Plant Biol.* **10**, 71.

Huis, R., Morreel, K., Fliniaux, O., Lucau-Danila, A., Fenart, S., Grec, S., Neutelings, G., Chabbert, B., Mesnard, F., Boerjan, W. and Hawkins, S. (2012) Natural hypolignification is associated with extensive oligolignol accumulation in flax stems. *Plant Physiol.* **158**, 1893–1915.

Jain, R., Lahiri, I. and Varma, A.J. (2000) Peanut stripe potyvirus: prevalence, detection and serological relationships. *Indian Phytopathol.* **53**, 14–18.

Kotake, T., Aohara, T., Hirano, K., Sato, A., Kaneko, Y., Tsumuraya, Y., Takatsuji, H. and Kawasaki, S. (2011) Rice Brittle culm 6 encodes a dominant-negative form of CesA protein that perturbs cellulose synthesis in secondary cell walls. *J. Exp. Bot.* **62**, 2053–2062.

Kumagai, M.H., Donson, J., della-Cioppa, G., Harvey, D., Hanley, K. and Grill, L.K. (1995) Cytoplasmic inhibition of carotenoid biosynthesis with virus-derived RNA. *Proc. Natl. Acad. Sci. USA*, **92**, 1679–1683.

Kvavadze, E., Bar-Yosef, O., Belfer-Cohen, A., Boaretto, E., Jakeli, N., Matskevich, Z. and Meshveliani, T. (2009) 30 000-year-old wild flax fibers. *Science*, **325**, 1359.

Lei, L., Li, S. and Gu, Y. (2012) Cellulose synthase complexes: composition and regulation. *Front Plant Sci.* **3**, 75.

Li, A., Xia, T., Xu, W., Chen, T., Li, X., Fan, J., Wang, R., Feng, S., Wang, Y., Wang, B. and Peng, L. (2013) An integrative analysis of four CESA isoforms specific for fiber cellulose production between *Gossypium hirsutum* and *Gossypium barbadense*. *Planta*, **237**, 1585–1597.

Liepman, A.H., Wightman, R., Geshi, N., Turner, S.R. and Scheller, H.V. (2010) Arabidopsis - a powerful model system for plant cell wall research. *Plant J.* **61**, 1107–1121.

Liu, E. and Page, J.E. (2008) Optimized cDNA libraries for virus-induced gene silencing (VIGS) using tobacco rattle virus. *Plant Methods*, **4**, 5.

Liu, Y., Schiff, M. and Dinesh-Kumar, S.P. (2002) Virus-induced gene silencing in tomato. *Plant J.* **31**, 777–786.

Ma, M., Yan, Y., Huang, L., Chen, M. and Zhao, H. (2012) Virus-induced gene-silencing in wheat spikes and grains and its application in functional analysis of HMW-GS-encoding genes. *BMC Plant Biol.* **12**, 141.

MacKinnon, I.M., Sturcova, A., Sugimoto-Shirasu, K., His, I., McCann, M.C. and Jarvis, M.C. (2006) Cell-wall structure and anisotropy in procuste, a cellulose synthase mutant of *Arabidopsis thaliana*. *Planta*, **224**, 438–448.

Mokshina, N., Gorshkova, T. and Deyholos, M.K. (2014) Chitinase-like (CTL) and cellulose synthase (CESA) gene expression in gelatinous-type cellulosic walls of flax (*Linum usitatissimum* L.) bast fibers. *PLoS ONE*, **9**, e97949.

Nairn, C.J. and Haselkorn, T. (2005) Three loblolly pine CesA genes expressed in developing xylem are orthologous to secondary cell wall CesA genes of angiosperms. *New Phytol.* **166**, 907–915.

Neutelings, G. (2011) Lignin variability in plant cell walls: contribution of new models. *Plant Sci.* **181**, 379–386.

Oomah, B.D. (2001) Flaxseed as a functional food source. *J. Sci. Food Agric.* **81**, 889–894.

Persson, S., Wei, H., Milne, J., Page, G.P. and Somerville, C.R. (2005) Identification of genes required for cellulose synthesis by regression analysis of public microarray data sets. *Proc. Natl. Acad. Sci. USA*, **102**, 8633–8638.

Richmond, T.A. and Somerville, C.R. (2000) The cellulose synthase superfamily. *Plant Physiol.* **124**, 495–498.

Rozen, S. and Skaletsky, H. (2000) Primer3 on the WWW for general users and for biologist programmers. *Methods Mol. Biol.* **132**, 365–386.

Ruiz, M.T., Voinnet, O. and Baulcombe, D.C. (1998) Initiation and maintenance of virus-induced gene silencing. *Plant Cell*, **10**, 937–946.

Ryu, C.M., Anand, A., Kang, L. and Mysore, K.S. (2004) Agrodrench: a novel and effective agroinoculation method for virus-induced gene silencing in roots and diverse Solanaceous species. *Plant J.* **40**, 322–331.

Saxena, I.M., Brown, R.M. Jr and Dandekar, T. (2001) Structure-function characterization of cellulose synthase: relationship to other glycosyltransferases. *Phytochemistry*, **57**, 1135–1148.

Senthil-Kumar, M. and Mysore, K.S. (2011) New dimensions for VIGS in plant functional genomics. *Trends Plant Sci.* **16**, 656–665.

Somerville, C. (2006) Cellulose synthesis in higher plants. *Annu. Rev. Cell Dev. Biol.* **22**, 53–78.

Sveinsson, S., McDill, J., Wong, G.K., Li, J., Li, X., Deyholos, M.K. and Cronk, Q.C. (2014) Phylogenetic pinpointing of a paleopolyploidy event within the flax genus (*Linum*) using transcriptomics. *Ann. Bot.* **113**, 753–761.

Tamura, K., Peterson, D., Peterson, N., Stecher, G., Nei, M. and Kumar, S. (2011) MEGA5: molecular evolutionary genetics analysis using maximum likelihood, evolutionary distance, and maximum parsimony methods. *Mol. Biol. Evol.* **28**, 2731–2739.

Thompson, J.D., Higgins, D.G. and Gibson, T.J. (1994) CLUSTAL W: improving the sensitivity of progressive multiple sequence alignment through sequence weighting, position-specific gap penalties and weight matrix choice. *Nucleic Acids Res.* **22**, 4673–4680.

Tian, J., Pei, H., Zhang, S., Chen, J., Chen, W., Yang, R., Meng, Y., You, J., Gao, J. and Ma, N. (2014) TRV-GFP: a modified Tobacco rattle virus vector for efficient and visualizable analysis of gene function. *J. Exp. Bot.* **65**, 311–322.

Valentine, T., Shaw, J., Blok, V.C., Phillips, M.S., Oparka, K.J. and Lacomme, C. (2004) Efficient virus-induced gene silencing in roots using a modified tobacco rattle virus vector. *Plant Physiol.* **136**, 3999–4009.

Velasquez, A.C., Chakravarthy, S. and Martin, G.B. (2009) Virus-induced gene silencing (VIGS) in *Nicotiana benthamiana* and tomato. *J. Vis. Exp.* **28**, 1292.

Venglat, P., Xiang, D., Qiu, S., Stone, S.L., Tibiche, C., Cram, D., Alting-Mees, M., Nowak, J., Cloutier, S., Deyholos, M., Bekkaoui, F., Sharpe, A., Wang, E., Rowland, G., Selvaraj, G. and Datla, R. (2011) Gene expression analysis of flax seed development. *BMC Plant Biol.* **11**, 74.

Voinnet, O. (2009) Origin, biogenesis, and activity of plant microRNAs. *Cell*, **136**, 669–687.

Wang, L., Guo, K., Li, Y., Tu, Y., Hu, H., Wang, B., Cui, X. and Peng, L. (2010) Expression profiling and integrative analysis of the CESA/CSL superfamily in rice. *BMC Plant Biol.* **10**, 282.

Wang, Z., Hobson, N., Galindo, L., Zhu, S., Shi, D., McDill, J., Yang, L., Hawkins, S., Neutelings, G., Datla, R., Lambert, G., Galbraith, D.W., Grassa, C.J., Geraldes, A., Cronk, Q.C., Cullis, C., Dash, P.K., Kumar, P.A., Cloutier, S., Sharpe, A.G., Wong, G.K., Wang, J. and Deyholos, M.K. (2012) The genome of flax (*Linum usitatissimum*) assembled de novo from short shotgun sequence reads. *Plant J.* **72**, 461–473.

Wijdeveld, M.M., Goldbach, R.W., Meurs, C. and van Loon, L.C. (1992) Accumulation of viral 126 kDa protein and symptom expression in tobacco systemically infected with different strains of tobacco mosaic virus *Physio*. *Mol. Plant Pathol.* **41**, 437–451.

Yoo, M.J. and Wendel, J.F. (2014) Comparative evolutionary and developmental dynamics of the cotton (*Gossypium hirsutum*) fiber transcriptome. *PLoS Genet.* **10**, e1004073.

Zhang, J.S., Zhao, J., Zhang, S. and He, C. (2014) Efficient gene silencing mediated by tobacco rattle virus in an emerging model plant physalis. *PLoS One*, **9**, e85534.

Zohary, D. and Hopf, M. (2004) *Domestication of Plants in the Old World*. New York: Oxford University Press.

Zuur, A.F., Ieno, E.N., Walker, N.J., Saveliev, A.A. and Smith, G.M. (2008) *Mixed Effects Models and Extensions in Ecology with R*. New York: S. Science.

Supporting information

Additional Supporting information may be found in the online version of this article:

Figure S1 qRT-PCR analysis of *LusCESA* genes in TRV2-*CESA3*-transformed plants.

Figure S2 Alignment of the 5 nucleotide fragments (bold) used for the VIGS constructions with the corresponding *LusCESA* sequences.

Table S1 Homology between the nucleotide sequences corresponding to the zone targeted by VIGS.

Table S2 qRT-PCR parameters for the specific amplification of 14 CESA transcripts.

Table S3 Primers used for TRV-based silencing constructions.